The phase diagram of charge-polydisperse colloids: a Monte Carlo study

1991 J. Phys.: Condens. Matter 3 7983

(http://iopscience.iop.org/0953-8984/3/40/019)

J. Phys.: Condens. Matter 3 (1991) 7983–7993. Printed in the UK

The phase diagram of charge-polydisperse colloids: a Monte Carlo study

B V R Tata and Akhilesh K Arora
Materials Science Division, Indira Gandhi Centre for Atomic Research, Kalpakkam 603 102, Tamil Nadu, India

Received 25 February 1991, in final form 2 July 1991

Abstract. The effect of charge polydispersity (CPD) on structural ordering of dilute charged aqueous colloidal suspensions is investigated using Monte Carlo simulations as a function of impurity-ion concentration (n_i) and CPD. The behaviours of the pair correlation function, mean square displacement and total interaction energy as functions of CPD and n_i are investigated to identify different phases. Crystalline order is found to transform into a glass-like order beyond a critical CPD. Both the crystalline and glassy orders are found to melt when n_i is increased. The transitions between the crystalline, glassy and liquid-like phases are characterized. The phase diagram as a function of CPD and n_i is reported. Colloidal crystals with finite CPD are found to melt at n_i lower than that corresponding to the monodisperse (zero-CPD) suspension. The behaviour of the phase boundaries is discussed.

1. Introduction

Unlike atomic systems, even the so-called monodisperse colloids have a certain degree of size and charge polydispersity. The effect of size polydispersity (SPD) on concentrated ordered colloids (both charged and uncharged) has been investigated extensively [1–5]. Monte Carlo (MC) simulations [3, 4] and density-functional theory of freezing [2] predict that crystallization disappears beyond a critical SPD, consistent with the simple model of Pusey [1] for hard-sphere systems. The effect of SPD on the structure factor, $S(Q)$, has also been investigated [5]. In concentrated suspensions, as hard-sphere interactions play a significant role in determining the structure, SPD influences the ordering more strongly than does charge polydispersity (CPD) [6]. However, in the deionized dilute charged colloids, where interparticle separation is typically several times the actual diameter, crystalline [7], liquid-like [8, 9] and glass-like [10–12] structural ordering is believed to arise due to the electrostatic interactions between charged species [13]. As the actual diameter does not play any role in determining the structure, the SPD has no effect on the ordering, as expected [14]. Instead, it is reasonable to expect CPD to play an important role in disrupting the crystalline order as the effective hard-sphere diameter is determined by the charge on the particle. Recently we have demonstrated using MC simulation that CPD beyond a critical value causes crystalline order to disappear, resulting in a glassy state [15]. Crystalline order of monodisperse colloids can also be made to disappear if the impurity-ion concentration n_i is increased in the suspension, causing melting of crystalline order into liquid-like order to occur. This happens due to the change in the

0953-8984/91/407983 + 11 $03.50

inverse Debye screening length [16, 17] as a function of n_i. Recently Kesavamoorthy *et al* [18] have measured the structure factor of dilute aqueous suspensions of polystyrene colloids close to the crystal–liquid interface, and reported that the height of the first peak in $S(Q)$, S_{max}, is 2.1 at melting, which is much lower than the corresponding value in atomic systems ($S_{max} \sim 2.85$). It has been conjectured that the lower value may arise due to CPD, as SPD is shown to have little effect on $S(Q)$ [18] for dilute suspensions. However, this has been confirmed neither experimentally nor theoretically. In view of these observations and conjectures, it is important to investigate the complete phase diagram of charge-polydisperse colloids in the CPD versus n_i plane.

In the present work we use the MC technique to simulate dilute aqueous charge-polydisperse colloidal suspensions. Although this technique lacks a strict or rigorous sense of timescale, we believe that it can still provide valuable insight into the properties of crystalline/glassy(amorphous)/liquid-like states of charge-polydisperse colloids. The effects of CPD on the crystallization and melting transition are investigated. From the simulations carried out for various values of CPD and n_i, the pair correlation function $g(r)$ and its Fourier transform $S(Q)$, the mean-square displacement (MSD), structural parameter R_g ($R_g = g_{min}/g_{max}$ where g_{min} is the value of the first minimum and g_{max} is first peak height in $g(r)$) and total interaction energy U_T are computed. From the behaviour of the above parameters, the crystalline, glassy and liquid-like phases are identified and the resulting phase diagram of charge-polydisperse colloids in the CPD versus n_i plane is reported.

2. Simulation details

MC simulations based on the Metropolis algorithm [19] for a canonical ensemble (constant NVT, where N, V and T are respectively the number of particles, the volume and the temperature) are carried out with periodic boundary conditions to simulate an aqueous colloidal suspension of polystyrene particles of diameter d (109 nm) interacting via a size-corrected Yukawa pair potential

$$U(r_{ij}) = Z_i Z_j e^2 [4 \exp(Kd)/(2 + Kd)^2] \exp(-Kr_{ij})/\varepsilon r_{ij}. \tag{1}$$

Here Z_i and Z_j are the charges (expressed in units of electronic charge e) on particles i and j respectively with a centre-to-centre distance of r_{ij}; K is the inverse Debye screening length given as $K^2 = 4\pi e^2(n_p\bar{Z} + n_i)/\varepsilon k_B T$ where $\bar{Z}$ is the average charge, k_B the Boltzmann constant, ε the dielectric constant of water, T the temperature (298 K) and n_i the monovalent impurity-ion concentration. $\bar{Z}$ is taken to be 600, which is the same as the value reported in [10]. In order to simulate a charge-polydisperse system, charges on the particles are assigned randomly from a symmetric rectangular distribution with mean $\bar{Z}$ and width 2Δ. The CPD is defined as the ratio of standard deviation to the mean, $(\overline{Z^2} - \bar{Z}^2)^{1/2}/\bar{Z}$ which in this case is $\Delta/\sqrt{3}\,\bar{Z}$. Simulations are done in a cubic cell, containing N particles ($N = 250$), of length L, which is fixed using the relation $L^3 = N/n_p$ to get the required particle concentration n_p. Starting configurations are always chosen as body-centred cubic (BCC) since at low volume fractions only the BCC structure has been found to be stable [7]. A step size of $0.5d$ is chosen such that trial rejection ratio is around 50%. The total interaction energy, U_T, is monitored to find out whether equilibrium has been reached or not. Approximately 6×10^5 configurations are discarded initially during which the system evolves to equilibrium.

A binary or a polydisperse system is often described in terms of number–number, charge–charge and number–charge correlations (Bhatia–Thornton structure functions) [20]. The experimentally measured scattered intensity is expressed in terms of these functions and form factors of the particles. As the system considered here consists of particles of identical size, but having different charges, the corresponding form factors for light scattering, which depend only on the size of the particles [9, 11], are also identical. This causes the terms corresponding to the charge–charge and number–charge structure functions to drop out from the expression of intensity or total structure factor [20], leaving only the term containing the number–number structure function. Hence, it is sufficient to describe the system in terms of number–number structure functions, $S(Q)$. This $S(Q)$ is calculated by Fourier transforming the number–number pair correlation function $g(r)$, which is obtained with an interval $\Delta r = 0.1\,d$ using the standard method [21], after reaching equilibrium, and averaging is done over 350 Monte Carlo steps (MCS). A MCS is defined as a set of N configurations during which on average each particle gets a chance to move.

Diffusion of particles is widely different in the suspensions with crystalline, glassy or liquid-like orders. In a polydisperse system it is expected to depend on the mass and size of the particle and also on the interaction with neighbours, which is determined by its charge. Although the mass and the size of all the particles are the same, differently charged particles may still diffuse differently. However, it is still meaningful to obtain an average MSD, which represents the diffusion in the polydisperse system. The average MSD is obtained using the expression

$$\overline{\langle r^2(m)\rangle} = \frac{1}{N}\sum_{i=1}^{N}[r_i(m+n) - r_i(n)]^2$$

where $r_i(m)$ is the position of ith particle after m MCS and the overbar denotes the averaging over initial configurations n.

Particle concentration is chosen to be $1.33 \times 10^{12}\,\mathrm{cm}^{-3}$ (volume fraction, $\varphi \sim 0.001$) because a dilute monodisperse colloidal suspension with liquid-like order at a similar concentration has been investigated experimentally as well as using MC simulations [13]. In order to see any possible system size effect, simulations are also carried out with $N = 432$ for various values of CPD at zero n_i. It is found that the results are essentially the same within statistical accuracy [15]. This is because of the strong screening, which causes the interaction potential at the cell boundary to drop by three orders of magnitude as compared to that at the nearest-neighbour separation. In order to see the sensitivity of the results to charge distribution, a Gaussian distribution has also been tried for a few values of CPD and n_i. The resulting structures were the same as those obtained using a rectangular distribution.

3. Results and discussion

As mentioned earlier, it is possible to make crystalline order disappear either by increasing polydispersity [15], which induces randomness in the system, or by increasing impurity-ion concentration [16, 17], which results in melting. Based on the behaviour

Table 1. Criteria for identifying crystalline (C), glassy (G) and liquid-like (L) states.

State	Structural ordering $g(r)$	Behaviour of MSD as a function of MCS
C	Long-range order	Saturation of MSD and root MSD $\ll a$
G	Short/medium-range order	Tendency towards saturation of MSD and root MSD $\ll a$
L	Short-range order	MSD varies linearly with time and root MSD may exceed a depending on time

$a = n_p^{-1/3}$ is the average interparticle separation.

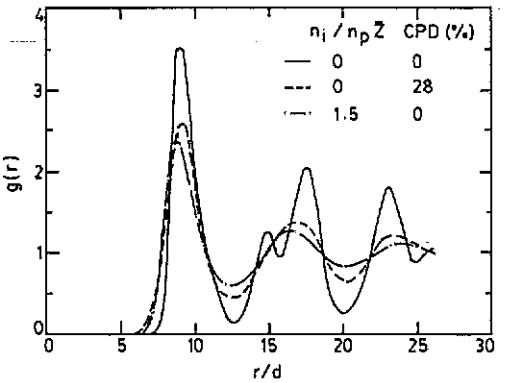

Figure 1. Pair correlation function for suspension with different charge polydispersities and impurity-ion concentrations for system with $n_p = 1.33 \times 10^{12}$ cm^{-3}.

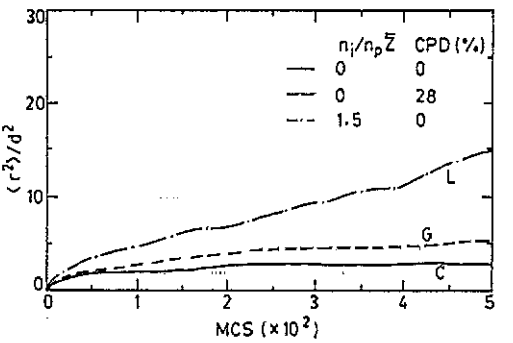

Figure 2. Mean-square displacement as a function of MCS for the suspension with the same parameters as in figure 1. The curves labelled C, G and L represent crystalline, glassy and liquid-like states respectively. Note the diffusive behaviour of the liquid-like state and the tendency towards saturation of the glassy and crystalline orders.

of particle diffusion and the range of structural ordering, crystalline, glassy and liquid-like states can be identified as given in table 1. Similar criteria for the identification of structural ordering on the basis of the behaviour of MSD with time have frequently been used earlier also [22].

Figure 1 shows the structure (pair correlation function) for deionized ($n_i = 0$) monodisperse suspension and those obtained for a suspension either with finite impurity or with finite CPD. Note that the BCC-like ordering (full curve) is destroyed either due to the presence of impurities at a concentration of $1.5 n_p \bar{Z}$ (chain curve) or due to the CPD of 28% (broken curve). The behaviour of the MSD as a function of MCS for these suspensions (the corresponding $g(r)$ curves are shown in figure 1) is shown in figure 2. From the disappearance of the characteristic crystalline peaks (chain curve in figure 1) and from the linear dependence of the MSD on MCS (chain curve in figure 2), it is straightforward to identify the system with $n_i = 1.5 n_p \bar{Z}$ with a liquid-like order. Similarly the disordered state at 28% CPD (broken curve in figure 1) can be assigned to a glassy order from the tendency of the MSD towards saturation (the slope, $d\langle r^2 \rangle / d(\text{MCS})$,

continuously decreases as a function of MCS and reaches a value close to that for a crystalline state) (broken curve in figure 2).

Although the $g(r)$ curves of the glassy and liquid-like ordered suspensions are qualitatively similar, it is worth pointing out the important differences between the two. Notice from figure 1 that the position of the first peak in $g(r)$ is shifted to lower r in the case of liquid-like order (chain curve) as compared to that of the crystalline $g(r)$, whereas it remains unshifted in the glassy state (broken curve). The liquid-like ordering is obtained by increasing n_i from 0 to $1.5n_p\bar{Z}$, whereas the glass is obtained by varying CPD from 0 to 28%. In the first case the Debye screening length (K^{-1}) decreases whereas in the latter case it remains constant and is the same as that in the crystalline order. The particles are more effectively screened when n_i is increased and hence they can approach closer, causing the peak in $g(r)$ to shift to lower r. The effect of n_i on the liquid-like ordering of a colloidal suspension interacting via a screened Coulomb potential has been investigated theoretically by Tata *et al* [23] using the rescaled mean spherical approximation (RMSA). The behaviour of the peak position with n_i obtained using the RMSA is qualitatively the same as observed in the present simulation. The distance of closest approach, i.e. the largest r for which $g(r)$ remains zero, which is smaller in the case of a liquid than it is in the crystalline order, also arises due to the change in K. On the other hand, the decrease in the distance of closest approach for the glassy order compared to that for the crystalline order arises because of the approach of particles with charges $Z_i < \bar{Z}$ closer to another particle also with $Z_j < \bar{Z}$.

3.1. Crystalline to glass (C → G) transition

It is evident from figures 1 and 2 that the C → G transition occurs at some CPD lower than 28%. In order to find out precisely the value of CPD at which the crystalline order disappears, simulations are carried out for different CPD values. Figure 3 shows the MSD at the end of M ($M = 500$) MCS as a function of CPD. Note that the MSD in suspensions with CPD > 26% are significantly higher than that in the systems with smaller CPD. As it is known that diffusion in glasses (non-crystalline solids) is much higher than that in crystalline counterparts, it is reasonable to assign the discontinuous increase in $\langle r_M^2 \rangle$ around 26% CPD to the C → G transition [15]. The $g(r)$ for a suspension with 28% CPD shown in figure 1 corresponds to a glassy structure just after this transition. For the sake of comparison, the effect of CPD on the diffusion of particles in a liquid-like ordered suspension ($n_i = 2.6n_p\bar{Z}$) is also shown in figure 3 as triangles. Note that the effect of CPD is weak and without any discontinuity and the $\langle r_M^2 \rangle$ is typically an order of magnitude larger compared to that in the solid, as expected. In order to discover how the critical CPD, at which the crystalline order disappears, varies with n_p, simulations are also carried out with $n_p = 1.33 \times 10^{13}$ cm^{-3} ($\varphi \sim 10^{-2}$) and the results are shown in figure 3. Note that the critical CPD increases from 26% to 32% when n_p is increased tenfold. As expected, the $\langle r_M^2 \rangle$ is correspondingly lower for larger n_p because the interparticle separation scales like $n_p^{-1/3}$. The increase in the critical CPD as n_p is increased can be understood as follows. As mentioned earlier in the case of dilute suspensions, instead of actual size, the effective hard-sphere diameter h, which is governed by the charge on the particle, determines the structural ordering. In this context it is meaningful to calculate effective hard-sphere diameters and effective size polydispersity (ESPD) for different CPD values. The largest r until which $g(r)$ remains zero in a monodisperse system represents the distance of closest approach for two particles and is taken to be h for a particle with charge $\bar{Z}$. The corresponding $h(Z)$ for a particle with any arbitrary

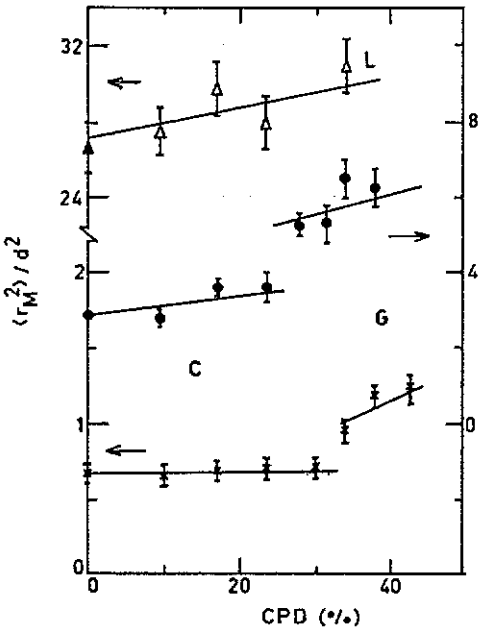

Figure 3. MSD at the end of M ($M = 500$) MCS as a function of CPD for different particle concentrations: (●) $n_p = 1.33 \times 10^{12}$ cm^{-3}; (×) $n_p = 1.33 \times 10^{13}$ cm^{-3}. The discontinuous increase in MSD at 26% for lower n_p and at 32% for higher n_p is associated with the C → G trnsition. The effect of CPD on liquid-like (L) order obtained at $n_p = 1.33 \times 10^{12}$ cm^{-3} and $n_i = 2.63 n_p \bar{Z}$ is also shown as triangles for the sake of comparison. Straight lines drawn through the points are guides to the eye.

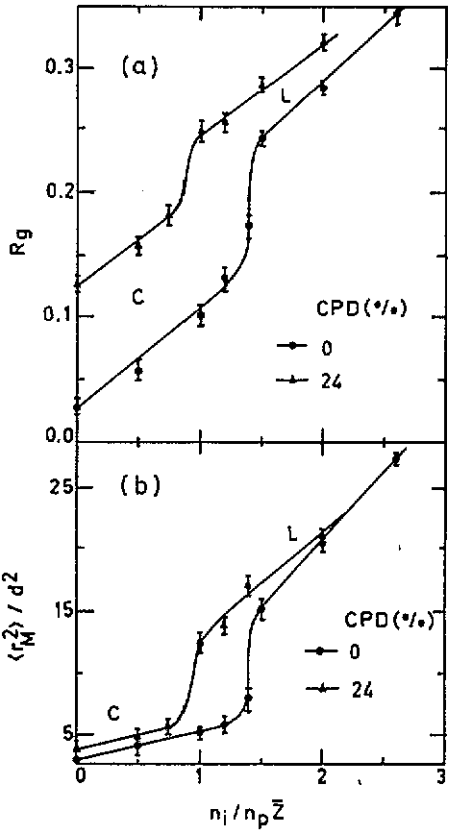

Figure 4. (*a*) MSD at the end of M ($M = 500$) MCS and (*b*) structural parameter R_g as function of n_i for different CPD for system with $n_p = 1.33 \times 10^{12}$ cm^{-3}: (●) 0 CPD; (▲) 24% CPD. The smooth curves drawn through the points are guides to the eye. Note that both $\langle r_M^2 \rangle$ and R_g exhibit discontinuous increase at $n_i = 1.45 n_p \bar{Z}$ for 0 CPD and at $0.9 n_p \bar{Z}$ for 24% CPD associated with the C → L transition.

charge Z is obtained using the procedure described earlier [15]. It is found that, although the critical CPD increases when n_p is increased, the corresponding ESPD ($17 \pm 1\%$) remains unchanged across the C → G transition. This critical ESPD may be compared with the value of 12% predicted for hard-sphere systems using a simple model [1]. The agreement appears fair in view of the simplicity of the procedure used to estimate $h(Z)$. Although in any such procedure one tries to estimate h, the presence of the interaction potential beyond h makes the actual system different from a true hard-sphere system. It is important to mention why the $g(r)$ of this glassy state does not exhibit a split second peak, which is often seen in simple monatomic solids, in metallic glasses and even in binary colloids [11]. It is known that splitting arises due to two topologically different positions of second neighbours and also leads to a split second peak in $S(Q)$. As more and more components constitute the glass, one does not expect to continue to observe

a split second peak. The splitting can get smeared out in a multicomponent system provided the randomness is beyond a certain critical value, which is dictated by the critical CPD or SPD of the system. If one rapidly cools the liquid with CPD or SPD to less than the critical value, the resulting glass can exhibit a split second peak in $g(r)$, but for liquids with CPD or SPD greater than the critical value, quenching yields a glassy state, which is expected to show a smooth second peak in $g(r)$.

3.2. Melting of charge-polydisperse colloidal crystal ($C \rightarrow L$)

The appearance of crystalline order in colloidal suspensions is known to occur due to the competition between interaction energy and thermal energy. It is convenient to define a dimensionless parameter $\Gamma = U_a/k_BT$ as the ratio of the interaction energy, U_a, at average interparticle separation a ($a = n_p^{-1/3}$) and the thermal energy k_BT. Melting of colloidal crystal occurs when Γ is less than a critical value Γ_c, which depends on n_p [24, 25]. Unlike atomic systems, where one varies Γ by varying the temperature, in aqueous colloidal suspensions it is possible to vary Γ at fixed T by changing n_i or n_p. The change in U_a is achieved by varying the inverse Debye screening length K, which depends on n_i and n_p. As the range of T variation is rather limited in aqueous colloidal suspensions, the relevant parameter for investigating melting/freezing of colloidal suspensions is the impurity-ion concentration. Previous investigations of melting/freezing have been done either using only a bare Yukawa potential (without goemetric factor in equation (1)) [25] or at zero n_i [24] with variation in Γ achieved by changing n_p (this is equivalent to dilution or compression). Instead, we have investigated melting as function of n_i, which is actually the parameter varied in all the experimental investigations, and also the effect of CPD on melting. In order to identify the melting transition uniquely, mean square displacement and structural parameter R_g (which represents the degree of structural correlation, a large value of R_g implying weaker structural correlation) are obtained for different values of n_i. Figure 4 shows $\langle r_M^2 \rangle$ and R_g as functions of n_i for a monodisperse suspension as well as for the one with finite CPD. Note that for the monodisperse suspension both $\langle r_M^2 \rangle$ and R_g increase discontinuously at $1.45 n_p \bar{Z}$, which could be unambiguously associated with the melting of crystalline order into a liquid-like order. Note that at melting $R_g \simeq 0.2$, which is the same as that obtained from computer simulation of Lennard-Jones systems by Raveche *et al* [26] and subsequently used for identifying melting/freezing in aqueous colloidal suspensions [24]. Figure 4 also shows the effect of CPD on melting of a charge-polydisperse colloidal crystal. Similar to the monodisperse suspension, the system with 24% CPD exhibits a discontinuous increase in $\langle r_M^2 \rangle$ and R_g across melting, but the magnitude of the jump is somewhat smaller. Note that $R_g \simeq 0.2$ for the melting of the polydisperse system also. It is important to point out that in this case melting occurs at $n_i = 0.9 n_p \bar{Z}$ instead of $1.45 n_p \bar{Z}$ corresponding to the monodisperse system. Also the effect of CPD is greater in the crystalline phase than in the liquid phase (curve drawn through points corresponding to zero and 24% CPD approach each other in the liquid phase whereas those in the crystalline phase are separated).

The Hansen–Verlet criterion for freezing [27] and Lindemann criterion for melting [28] have been extensively used to identify melting/freezing in computer experiments [29]. The applicability of these criteria to colloidal suspensions has also often been re-examined [18, 24, 25]. Molecular dynamics experiments [25] confirm that the Hansen–Verlet criterion, i.e. liquid freezes into crystalline solid when the height of the first peak in the structure factor is around 2.85, does apply in the case of colloidal suspensions; however, Kesavamoorthy *et al* [18] have reported $S_{max} \sim 2.1$ close to the colloidal-liquid/

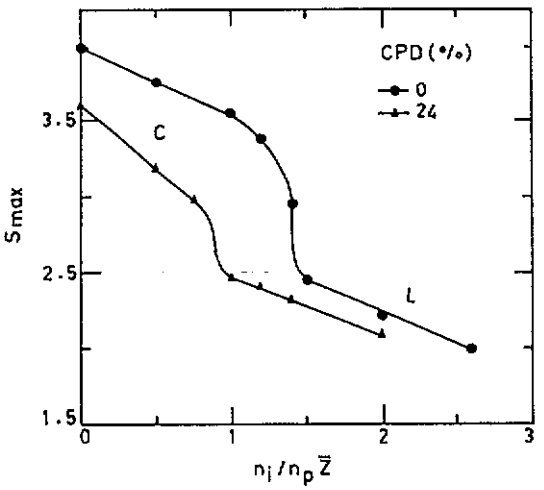

Figure 5. Height of first peak in structure factor S_{max} as a function of n_i for different CPD: (●) 0 CPD; (▲) 24% CPD. Smooth curves drawn through the points are guides to the eye. Note that the discontinuous change in S_{max} associated with the C → L transition occurs at the same n_i as in figure 4.

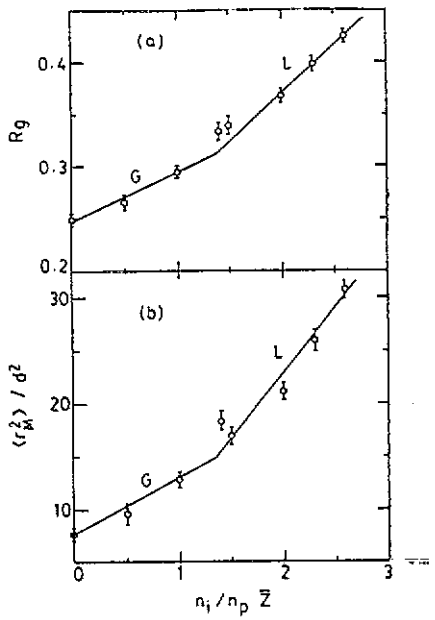

Figure 6. (*a*) The structural parameter R_g and (*b*) the MSD at the end of M ($M = 500$) MCS as a function of n_i for glass-like ordered suspension with 34% CPD. Note the change in slope of R_g as well as $\langle r_M^2 \rangle$ at around $n_i = 1.45 n_p \bar{Z}$ indicating glass (G) to liquid (L) transition.

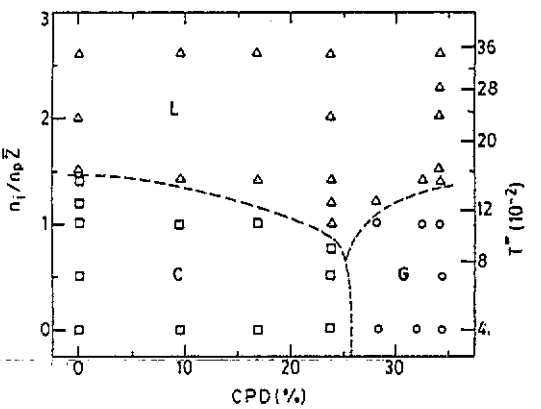

Figure 7. The phase diagram (CPD versus n_i) for the charge-polydisperse system with $n_p = 1.33 \times 10^{12}$ cm^{-3}. Symbols □, ○ and △ represent crystalline (C), glassy (G) and liquid-like (L) regions respectively. The broken curves representing the phase boundaries are guides to the eye. The equivalent temperature T^* corresponding to n_i is also marked on the y axis (see text).

colloidal-crystal coexistence boundary. It was conjectured that the CPD in the colloidal suspension could be the reason for S_{max} being low. In order to see the effect of CPD on S_{max} across melting, we calculate $S(Q)$ by Fourier transforming $g(r)$. Figure 5 shows the

dependence of S_{max} on n_i for a monodisperse suspension and that for a suspension with largest possible CPD (24%) for which a crystalline order can exist. Note the discontinuities across the melting transition and S_{max} being as high as 2.5 in the monodisperse as well as charge-polydisperse liquids; hence CPD cannot account for the lowering of S_{max} to 2.1 at freezing; one has to look for other possible reasons.

Melting is often investigated in the context of the Lindemann criterion, which states that solids should melt when the ratio of root MSD to the lattice spacing exceeds a certain value W. For atomic systems the value of W is 0.1; however, for colloidal crystals [24] it has been reported to be 0.23. The present simulation results yield $W = 0.28 \pm 0.05$ consistent with that reported earlier. Recently the effect of finite system size on the MSD of crystals using Lennard-Jones, Yukawa (uncorrected for size) and r^{-n} interactions has been investigated in the context of the use of Lindemann criterion for melting [30]; however, such studies are not available for the size-corrected Yukawa potential. In view of this, the value of W at melting, obtained in the present work using finite system size, could be slightly different from that corresponding to an infinite system. A much larger value of W essentially implies that colloidal crystals can sustain much larger amplitudes of motion of particles than in atomic solids. The larger value in colloids could be due to the shallowness of the potential well formed by neighbours (because interaction is soft and softness is determined by Debye screening length), which is different from the case in atomic solids.

3.3. Melting of glass ($G \rightarrow L$)

In analogy with the melting of crystalline order, it is resonable to expect a glassy order to melt upon increasing the impurity-ion concentration. As both the glassy and the liquid-like states are disordered, one does not expect sharp discontinuities in R_g and $\langle r_M^2 \rangle$ in this case, as noted earlier for melting of colloidal crystals. Figure 6 shows these quantities as a function of n_i for a suspension with 34% CPD. Note the change of slope in R_g and $\langle r_M^2 \rangle$ around $n_i = 1.45 n_p \bar{Z}$ which could be associated with the melting of glass. A similar change of slope in R_g as a function of temperature, to which a Lennard-Jones liquid is quenched, has been used earlier to identify the glass transition by Wendt and Abraham [31]. The value of R_g at which the glass transition took place was found to be 0.14 whereas the present results for charge-polydisperse glass yield a value ~0.3. Similarly, glasses obtained by rapid cooling of liquid exhibited $S_{max} > 2.85$ or equivalently $g_{max} > 2.55$ [31], whereas g_{max} is found to be only 2.22 for a charge-polydisperse glass. The value of $R_g = 0.14$ at the glass transition being lower than $R_g = 0.2$ at freezing (into crystalline order) is understandable as the glass transition temperature T_g is always lower than the freezing temperature T_f. The same argument holds for $S_{max} > 2.85$ or $g_{max} > 2.55$ for glasses produced by quenching. The value of R_g or g_{max} in the case of charge-polydisperse glass being significantly different from those in quenched glasses suggests that the two types of glasses are fundamentally different. At CPD > 26% the simulations show that BCC structure is unstable and the system evolves into a glassy structure. This suggests that the CPD glass is more stable than the corresponding BCC crystalline state. In order to confirm whether a CPD glass is in a true ground state or not, one has to demonstrate that the free energy of the disordered structure (glass) is lower than those of various possible crystalline phases, which is rather time-consuming. As mentioned in section 3.1, the charge-polydisperse system can be mapped onto an effective hard-sphere system. Different charges on the particles lead to a variety of hard-sphere diameters. Incompatibility of packing (i.e. size-mismatch frustration) of these

hard spheres in a crystalline state leads to a glassy order. Thus a charge-polydisperse glass can be considered somewhat analogous to a spin glass, which also has frustrated spins due to random interaction. Apart from the conventional method of quenching of the liquid-like phase, CPD and similarly SPD provides another way of obtaining the glassy state; however, this route is not available in the case of atomic systems.

3.4. Phase diagram

Having identified the crystalline (C), liquid-like (L) and glassy (G) phases and having characterized the transitions between these, one can now construct the phase diagram of a charge-polydisperse colloidal system, which is shown in figure 7. Note that it consists of three regions, viz. the crystalline phase for low CPD and low n_i, a glassy state for high CPD and low n_i and a liquid-like region for high n_i. As the variation of n_i causes the nearest-neighbour interaction energy U_a to change, one can define a reduced temperature $T^* = k_BT/U_a$, which expresses the thermal energy in units of the interaction energy. The reduced temperature T^* thus obtained is also marked on the y axis in figure 7. However, there is no thermodynamic parameter analogous to the CPD.

Note from figure 7 the behaviour of the crystal–liquid phase boundary, which suggests that melting of colloidal crystals with finite CPD occurs at a lower n_i than that corresponding to a monodisperse suspension. This can be understood if one uses the concept of reduced temperature T^*. A decrease in n_i implies an increase in U_a, or equivalently a decrease in T^*; the present results suggest that the melting occurs at a lower T^* for a system with finite CPD. As noted earlier, the value of R_g at melting being independent of CPD implies that a colloidal crystal melts when structural correlations become weaker than a certain value irrespective of the CPD. In a suspension with finite CPD, apart from the thermal fluctuations ($\sim k_BT$) the randomness due to charge also contributes to R_g, and hence at finite CPD melting can occur when the thermal contribution to randomness is smaller in magnitude, i.e. at a lower T^*. Furthermore, note that the glass–liquid phase boundary shows a rising trend when CPD is increased. It is reasonable to expect that the glass obtained with higher and higher CPD beyond the critical CPD will be more stable against the formation of a crystalline state. The better stability of the glassy order away from the C → G boundary makes it melt at higher T^*. The boundary for C → G transition at finite n_i is obtained by smoothly joining the C → L boundary to the point of the critical CPD corresponding to the C → G transition at zero n_i. It is worth mentioning that the phase boundaries shown in figure 7 represent the points of instability of crystalline phase to the formation of liquid or glassy phases. It is likely that the reverse transitions may not take place at the same points in the phase diagram (hysteresis effects).

Finally, it would be of further interest to investigate the order of the C → G transition and also to explore any possible regions of coexistence. Investigations of these aspects of the phase transition would require much larger system size, typically a thousand particles or above.

4. Conclusions

To conclude, crystalline order of a dilute aqueous colloidal suspension can be made to disappear either by increasing n_i (liquid-like order) or by increasing the polydispersity of the charge on the particle (glassy order). Although the critical CPD for C → G transition depends on the volume fraction, the polydispersity of effective hard-sphere diameter

remains essentially constant. Melting of colloidal crystals occurs when $U_T \sim 25k_BT$. A charge-polydisperse system melts at lower impurity concentration than a monodisperse system. The structural parameter R_g, which is a measure of randomness in the system (both thermal as well as that arising due to CPD), remains constant across melting. The large magnitude of MSD in colloidal crystals close to melting compared to that in atomic systems is probably due to the softness of the potential.

Acknowledgments

The authors wish to thank Dr K Krishan for his keen interest in the work.

References

[1] Pusey P N 1987 *J. Physique* **48** 709
[2] Barrat J L and Hansen J P 1986 *J. Physique* **47** 1547
[3] Dickinson E and Parker R 1985 *J. Physique Lett.* **46** L229
[4] Dickinson E, Parker R and Lal M 1981 *Chem. Phys. Lett.* **79** 578
[5] van Beurten P and Vrij A 1981 *J. Chem. Phys.* **74** 2744
[6] Senatore G and Blum L 1985 *J. Phys. Chem.* **89** 2676
[7] Williams R and Crandall R S 1974 *Phys. Lett.* **48A** 225
[8] Pusey P N 1979 *Phil. Trans. R. Soc.* A **293** 429
[9] Tata B V R, Kesavamoorthy R and Sood A K 1987 *Mol. Phys.* **61** 943
[10] Lindsay H M and Chaikin P M 1982 *J. Chem. Phys.* **76** 3774
[11] Kesavamoorthy R, Sood A K, Tata B V R and Arora A K 1988 *J. Phys. C: Solid State Phys.* **21** 4737
[12] Yoshimura S and Hachisu S 1985 *J. Physique Coll.* **46** C3 115
[13] Tata B V R, Sood A K and Kesavamoorthy R 1990 *Pramana–J. Phys.* **34** 23
[14] Dickinson E 1979 *J. Chem. Soc. Faraday Trans.* II **75** 466
[15] Tata B V R and Arora A K 1991 *Europhys. Lett.* submitted
[16] Hachisu S, Kobayashi Y and Kose A 1973 *J. Colloid Interface Sci.* **42** 342
[17] Sirota E B, Ou-Yang H D, Sinha S K and Chaikin P M 1989 *Phys. Rev. Lett.* **62** 1524
[18] Kesavamoorthy R, Tata B V R, Arora A K and Sood A K 1989 *Phys. Lett.* **138A** 208
[19] Binder K 1979 *Monte Carlo Methods in Statistical Physics* ed K Binder (New York: Springer) p 1
Hansen J P and McDonald I R 1986 *Theory of Simple Liquids* 2nd edn (London: Academic)
[20] Waseda Y 1980 *The Structure of Non-Crystalline Materials* (New York: McGraw-Hill)
[21] Rahman A 1964 *Phys. Rev.* **136** A405
[22] Rosenberg R O, Thirumalai D and Mountain R D 1989 *J. Phys.: Condens. Matter* **1** 2109
[23] Tata B V R, Kesavamoorthy R and Arora A K 1986 *Mol. Phys.* **57** 369
[24] Rosenberg R O and Thirumalai D 1987 *Phys. Rev.* A **36** 5690
[25] Robbins M O, Kremer K and Grest G S 1988 *J. Chem. Phys.* **88** 3286
[26] Raveche H J, Mountain R D and Streett W B 1974 *J. Chem. Phys.* **61** 1970
[27] Hansen J P and Verlet L 1969 *Phys. Rev.* **184** 151
[28] Lindemann F A 1910 *Z. Phys.* **11** 609
[29] Levesque D, Weis J J and Hansen J P 1979 *Monte Carlo Methods in Statistical Physics* ed K Binder (New York: Springer) p 47
[30] Robbins M O, Grest G S and Kremer K 1990 *Phys. Rev.* B **42** 5579
[31] Wendt H R and Abraham F F 1978 *Phys. Rev. Lett.* **41** 1244